Silver nanocubes

Sublimation-Induced Shape Evolution of Silver Cubes**

*Yong Ding, Fengru Fan, Zhongqun Tian, and Zhong Lin Wang**

Surface free energy is a criterion usually employed to identify the stability of a solid surface. Nanoparticles of face-centered cubic (fcc) noble metals are usually enclosed by the lower-energy surfaces such as {111} and {100}, because these surfaces are believed to have the lowest energy, typically following $\gamma\{111\}<\gamma\{100\}<\gamma\{110\}$.[1,2] This criterion is proposed based on the assumption that the surface free energy is largely determined by the coordination number of the surface atoms at the top layer, which in general can explain the formation of various metal nanoparticles such as Au, Pt, and Ag. However, one of the simple manifestations of the presence of a surface is the relaxation of atoms located at the first, second, and even deeper surface layers, either inwards or outwards with respect to bulk terminated positions, which can contribute to the surface free energy in a realistic situation. As a result of surface relaxation that may sensitively depend on temperature, the surface free energy could be dramatically minimized. Due to the high density of surface atoms and their relatively high coordination numbers, both experiments and theoretical calculations manifest that relaxations of metal {111} surfaces at room temperature are expected to be minimal.[2] Low-energy electron diffraction (LEED)[3] and high-energy ion-scattering (HEIS)[4] studies found that oscillatory relaxation of the interlayer spaces occurred in {110} surfaces.

With the increase of temperature, the contribution of the lattice vibration to the surface free energy increases. As we know, the creation of a crystal surface means breaking of bulk translational symmetry, which implies that an anharmonic behavior of the restoring forces should be expected. Such anharmonic effects become increasingly crucial to the surface stability when the temperature is close to the melting point, such as the unexpected large thermal expansion of the Ag {111} surface.[5] Although some controversies existed in the early stages of theoretical understanding,[6–8] surface-vibration-enhanced anharmonicity does exist. In their medium-energy ion-scattering experiment, Statiris et al.[5] found that the first interlayer spacing of Ag {111} is contracted at temperatures below 670 K, but increases at higher temperatures in a nonlinear fashion and is expanded by ≈10% at 80 K below the melting point. Furthermore, a surface free energy as high as 7.2 J m^{-2} of spherical Ag nanoparticles was retrieved by fitting the evaporation data with the Kelvin effect,[9] while the surface free energy of bulk Ag at room temperature is just in the range of 1.065 to 1.54 J m^{-2}.[10]

Based on the anharmonic perturbation theory, the ratio of atomic vibrations between surface and bulk atoms can be calculated. According to Lindemann's melting criterion,[11] the anisotropic surface melting was predicted. Taking Ag as an example, the melting points of {110}, {100}, and {111} surfaces are 887, 906, and 966 K, respectively.[12] After taking account of the multilayer relaxation effect, the theory by Jayanthi et al. leads to a reversed order in which the low-index surfaces of metals are predicted to become unstable, from {110}–{100}–{111} to {111}–{100}–{110}.[13,14] To date, although a lot of work has been carried out to study the thermal behavior of fcc metal surfaces,[15–19] it is still unclear whether the {111} surface is the stable one or not at high temperature.

To clarify which surface in fcc metals is the thermally stable one at high temperature, we designed an in situ sublimation experiment using silver as the target metal for its comparably high vapor pressure.[20,21] If a surface automatically forms during the evaporation process, it must be energetically favorable. Our original Ag nanoparticles were {100} surfaces enclosed cubes of dimension ≈100 nm. During the sublimation process, to our surprise the {110} surfaces were the only stable and well-defined surfaces observed at high temperature, whereas {100} and {111} surfaces were not stable and shrank at high temperature. This experimental study proves the theoretical prediction.

Figure 1 shows three bright-field transmission electron microscopy (TEM) images recorded from the same area but at different temperatures. The selected-area electron diffraction (SAED) pattern of the outlined cube is displayed as an inset in Figure 1a. It is obvious that the Ag particles are almost perfect cubes enclosed by {100} surfaces at room temperature. The dimension of these cubes varies from 60 to 110 nm, while the dominant size is ≈100 nm. The tracked sublimation process revealed that two different sublimation scenarios existed. In the first scenario, when the Ag cube started to lose mass and volume, the whole cube was completely sublimed in less than

[*] Prof. Z. L. Wang, Dr. Y. Ding
School of Materials Science and Engineering
Georgia Institute of Technology
Atlanta, GA 30332-0245 (USA)
E-mail: zhong.wang@mse.gatech.edu
F. R. Fan, Prof. Z. Q. Tian
Department of Chemistry
Xiamen University
Xiamen 361005 (P. R. China)

[**] This research was supported by DARPA (Army/AMCOM/REDSTONE AR, W31P4Q-08-1-0009), BES DOE (DE-FG02-07ER46394), the Air Force Office (FA9550-08-1-0446), DARPA/ARO W911NF-08-1-0249, KAUST Global Research Partnership, the World Premier International Research Center (WPI) Initiative on Materials Nanoarchitectonics, MEXT (Japan), and NSF (DMS 0706436, CMMI 0403671). F.R.F. is grateful for the fellowship from the China Scholarship Council (CSC, No. 20073020).)

DOI: 10.1002/smll.200901189

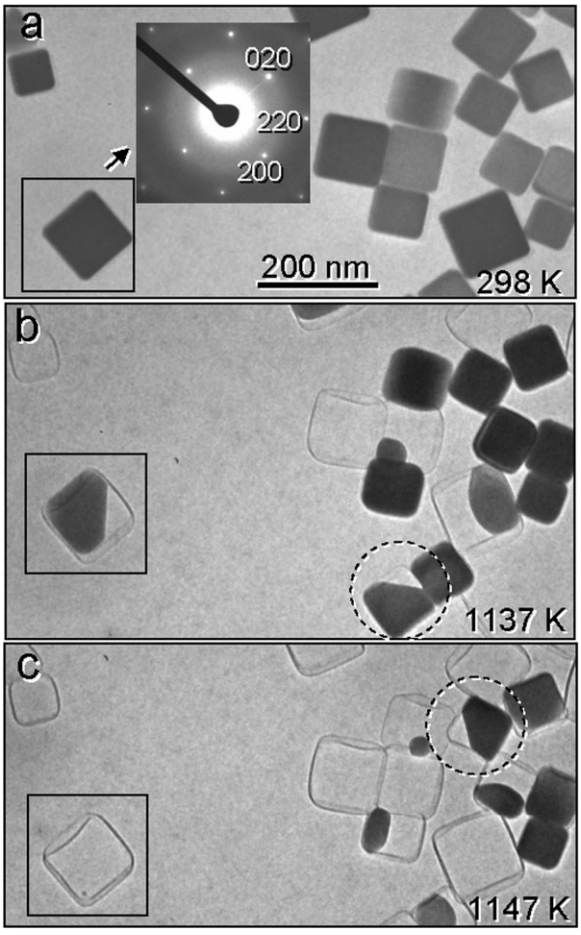

Figure 1. a–c) Bright-field TEM images of Ag cubes recorded at 298, 1137, and 1147 K, respectively. The inset in (a) is a SAED pattern from the outlined Ag cube. Some cubes that show {110} surfaces are enclosed by circles in (b) and (c).

10 min and the volume loss was symmetric at each surface. In the second scenario, such evaporation was much slower and one or more {100} surfaces of the cube were adhered on the carbon capping shell, which was decomposed from polyvinylpyrrolidone (PVP) surfactant at high temperature. Within 66 min, the sample temperature was increased from 298 to 1137 K. As shown in Figure 1b, some Ag cubes were completely sublimed before the temperature reached 1137 K and only the capping shells were left, which can be attributed to the first scenario. The sublimation of the outlined cube started from one corner and later showed a well-developed large {110} surface at 1137 K. The detailed sublimation process of this second-scenario cube is displayed in Figure 2 in a temperature sequence. With the temperature further increased to 1147 K in 15 min, most of the cubes were sublimed. With much care, after tracking more than 20 Ag cubes belonging to the second slow-sublimation scenario, we found that they always showed well-defined {110} surfaces in one stage during the temperature increase. The circles in Figure 1b and c give some more examples.

If there was no serious substrate effect, an Ag spherical particle with radius ≈42 nm would be completely evaporated in less than 10 min at 1026 K under a pressure of 2.7×10^{-4} Pa.[21] In our experiment as described in Figure 1, the vacuum in our TEM chamber was much better (3×10^{-6} Pa) and the sample temperature was higher. The two different scenarios of the sublimation processes mentioned above can be considered as due to weak and strong substrate interaction, respectively. However, their triggering temperatures to start the volume loss are different although their sizes are comparable. We can explain such a phenomenon as follows. Firstly, with the decomposition of the PVP surfactant above 620 K,[22,23] the carbon capping shell may seal the Ag cube fairly well, and thus the local pressure surrounding the Ag nanoparticle could be higher than that in the TEM chamber. With the increase of temperature, the pressure in the carbon capping shell would be built up as a result of surface sublimation. Due to the different degree of perfection and thickness of each capping shell, the pressures they can hold are different. At a certain temperature, the breaking of their capping shells would trigger a speedy sublimation, as characterized by the volume loss. After that, the interaction between the Ag nanoparticle and carbon shell determines which scenario the sublimation belongs to.

The whole sublimation process of the outlined Ag cube in Figure 1 was tracked and displayed in Figure 2 in a time sequence. Its slow evaporation rate suggests that the interaction between the cube and carbon-shell substrate is fairly strong. The expansion of the size shown in Figure 2b seems mainly due to the tilting of the cube on the TEM grid. The asymmetric contrast of the cube meant a loss in local mass/volume. From 1116 to 1137 K, as a result of more mass loss, the contrast of the whole cube became weak and some free spaces between the cube and the capping shell were observed. Although the roughening could be observed at least at the side surfaces of the cube (the side surfaces are not perfectly flat), the {100} surfaces were still kept by the cube. Upon keeping at 1137 K for 216 s, with the elimination of the {100} surfaces on the right-hand part of the cube, a {110} side surface was built up during the evaporation as shown in Figure 2d. With further sublimation, the {110} surface was replaced step by step with a spherical surface (Figure 2e and f). After the particle size was smaller

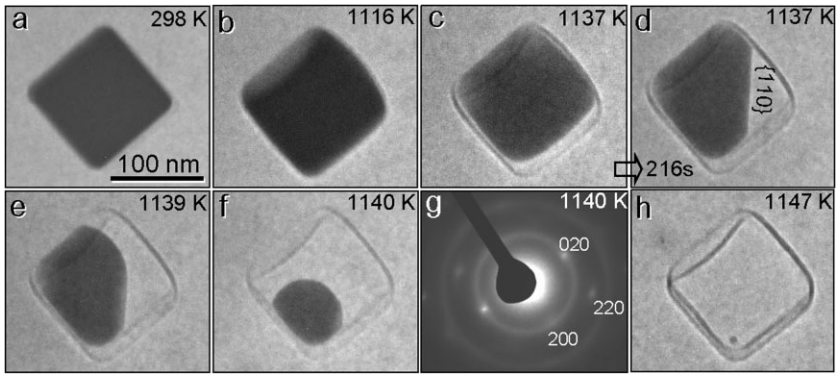

Figure 2. In situ bright-field TEM images showing the full sublimation process of an Ag cube (outlined in Figure 1). The temperature at which each image was recorded is indicated.

than 50 nm, except for the capping-shell-locked {100} surfaces, the other part of the surface became spherical (Figure 2f). Figure 2h shows the SAED pattern of the spherical nanoparticle in Figure 2f. The main body of the nanoparticle is still crystalline, although surface melting could be possible. With further development of sublimation, the final particle shrank to 5 nm in diameter as shown in Figure 2h, and then the sublimation stopped due to the oxidization of the Ag nanoparticle (not discussed here). The nonsymmetric truncation of the {110} surface around the particle is most likely due to the effect from the substrate. The other shapes shown in Figure 1b and c are just the in-between shapes of the Ag cube during its shape evolution (Figure 2).

During the entire sublimation process as described in Figure 2, the {110} surface is the only surface automatically developed in the shape evolution. Compared with {100} surfaces, {110} surfaces are much more stable. If {111} surfaces did exist, the TEM diffraction contrast would give us some evidence, but we did not observe them. Due to the carbon shell capped on the silver cube, the surface free energy of those {100} surfaces may be modified. However, such capping shells were well separated from the newly developed {110} surfaces, as we observed in Figures 1 and 2, and the size of the capping shell was almost fixed, while the Ag cube diminished as the result of sublimation. Therefore, the surface absorption effect on {110} surfaces introduced by the capping shell can be reasonably ignored.

Figure 3 shows the sublimation process of Ag cubes that belong to the second scenario for which the substrate effect can be ignored. The shape effect around a (200) diffraction spot recorded at room temperature from an Ag cube is displayed in Figure 3d, in which the streaking along the ⟨100⟩ direction is due to the existence of the {100} surfaces. Upon increasing the temperature to 1026 K (Figure 3a), the cubes became truncated and their {110} surfaces instead of {111} surfaces were developed from the corners of the cubes. The (200) diffraction spot recorded from the top-left cube is displayed in Figure 3e. The reduced ⟨100⟩ streaking intensity and the appearance of ⟨110⟩ streaking further confirm the formation of {110} surfaces. Figures 3a and b were recorded 10 min apart, and simultaneously the temperature was increased to 1095 K. The small cube enclosed by a circle was completely sublimed. The (200) diffraction spot from the top-left cube in Figure 3b is displayed in Figure 3f, which gives stronger ⟨110⟩ streaking. Due to its comparably smaller size, the bottom-right cube shows better diffraction contrast in Figure 3b, and its magnified image is further displayed in Figure 3c. Based on the contrast that is mainly contributed by the projected mass/thickness, we can work out the three-dimensional shape of the cube. The central dark area corresponds to the top and bottom {100} surfaces, whilst the weak contrast from the surrounding areas comes from inclined {110} surfaces. The dark edges along ⟨111⟩ directions can be distinguished as well, which is indicated by the arrows in Figure 3c. The area in between the two dashed lines may correspond to the formation of a {111} surface, although it is also possibly due to the top and bottom edges (such edges are the boundaries of the top and bottom two connected {110} surfaces) not being in the same plane. There is no doubt that {110} are the dominant surfaces. The shape of the cube in

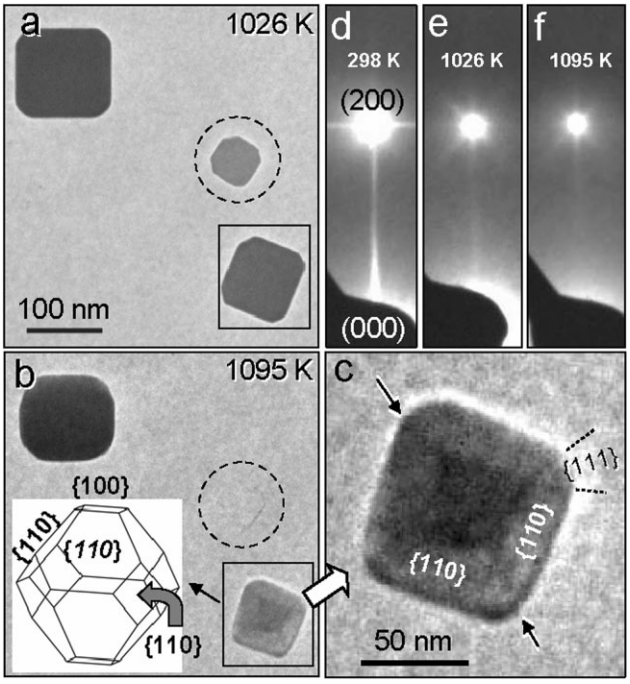

Figure 3. a,b) Bright-field TEM images of three Ag cubes recorded at 1026 and 1095 K, respectively. c) Magnified image of the bottom-right cube in (b). Arrows: dark edges along ⟨111⟩ directions. d–f) The (200) diffraction spots in the SAED patterns recorded at 298, 1026, and 1095 K, respectively. The diffraction pattern is enlarged so that it shows only the (200) spot and the central transmitted (000) spot (blocked by beam stopper), for presenting the shape effect around the (200) diffraction spot.

Figure 3c can be considered as a truncated octahedron with {110} and {100} as its surfaces. A sketch of the cube is shown in the inset of Figure 3b. Generally, the Ag nanocubes with sizes larger than 50 nm prefer to expose their {110} surfaces at high temperature, these surfaces being produced by a sublimation process.

The melting temperature T_m of silver is 1234 K.[24] The stable {110} surfaces were observed in a temperature range of 0.83 to 0.92 T_m in our in situ experiments. According to Chatterjee's calculation,[12] the melting points of {111}, {100}, and {110} surfaces of silver are 0.78, 0.73, and 0.72 T_m, respectively. The predicted stable surface at high temperature is {111}, but not {110}. The inconsistency between our experimental results and the prediction suggests that only considering the anharmonic effect in the first surface layer is not sufficient for illustrating the surface stability. After introducing multilayer relaxation, the calculated instability temperature of {110} can reach 0.97 T_m in the copper system.[13] Also as predicted by multilayer relaxation, compared with {111} and {100} surfaces, {110} surfaces are thermally more stable at temperatures close to the melting point. This expectation is proved by our experiments.

Another phenomenon worth emphasizing is that the free surface of Ag nanoparticles is spherical when the size shrinks to under 50 nm (Figure 2). The effect of size on the melting point has been well studied.[25] However, the critical size of silver nanoparticles below which the melting point can dramatically change is ≈2 nm.[24]

In summary, the sublimation process of silver cubes, enclosed by {100} surfaces and ≈100 nm in size, was investigated by in situ TEM. At an Ag nanoparticle size larger than 50 nm, the sublimation-induced stable surface is the {110} surface rather than the conventional {111} and {100} surfaces, in agreement with the theoretical prediction of Jayanthi et al. This finding is rather surprising.

Experimental Section

The Ag nanocubes used for the experiments were synthesized by modifying the previously reported method.[26] PVP solution (5 mL, 0.375 M in ethylene glycol (EG)) was prepared in a 50-mL three-neck round-bottomed flask and the solution was heated at reflux in an oil bath at 173 °C for 5 min. After that, NaCl solution (0.15 mL, 0.020 M in EG) was added. $AgNO_3$ solution (2.5 mL, 0.125 M in EG) was injected under vigorous stirring into the hot solution using a syringe pump (PHD 2000, Harvard Apparatus Co.) at a rate of 0.125 mL min^{-1}. Finally, the reaction mixture was kept at the same temperature for an extra 7 h.

The in situ work was carried out by using a Hitachi HF2000 transmission electron microscope operated at 200 kV. The TEM samples were prepared by depositing drops of the Ag nanotube solution onto carbon-coated nickel grids, followed by automatic drying in air. A heating stage from Gatan Company was used to heat the sample to as high as 1200 K. The vacuum in the TEM chamber was kept at 3×10^{-6} Pa. The images and diffraction patterns were recorded by a CCD camera to track the structural evolution during heating.

Keywords:
nanocubes · silver · sublimation · surfaces · transmission electron microscopy

[1] Z. L. Wang, *J. Phys. Chem. B* **2000**, *104*, 1153.
[2] K. P. Bohnen, K. M. Ho, *Surf. Sci. Rep.* **1993**, *19*, 99.
[3] H. L. Davis, J. R. Noonan, *Surf. Sci.* **1983**, *126*, 245.
[4] I. Stensgaard, R. Feidenhansl, J. E. Sorensen, *Surf. Sci.* **1983**, *128*, 281.
[5] P. Statiris, H. C. Lu, T. Gustafsson, *Phys. Rev. Lett.* **1994**, *72*, 3574.
[6] A. N. Al-Rawi, A. Kara, P. Staikov, C. Ghosh, T. S. Rahman, *Phys. Rev. Lett.* **2001**, *86*, 2074.
[7] A. Kara, P. Staikov, A. N. Al-Rawi, T. S. Rahman, *Phys. Rev. B* **1997**, *55*, 13440.
[8] J. J. Xie, S. de Gironcoli, S. Baroni, M. Scheffler, *Phys. Rev. B* **1999**, *59*, 970.
[9] K. K. Nanda, A. Maisels, F. E. Kruis, H. Fissan, S. Stappert, *Phys. Rev. Lett.* **2003**, *91*, 106102.
[10] J. R. Smith, A. Banerjea, *Phys. Rev. Lett.* **1987**, *59*, 2451.
[11] C. L. Lindemann, *Phys. Z.* **1911**, *12*, 1197.
[12] B. Chatterjee, *Nature* **1978**, *275*, 203.
[13] C. S. Jayanthi, E. Tosatti, A. Fasolino, L. Pietronero, *Surf. Sci.* **1985**, *152*, 155.
[14] C. S. Jayanthi, E. Tosatti, L. Pietronero, *Phys. Rev. B* **1985**, *31*, 3456.
[15] D. L. Adams, H. B. Nielsen, J. N. Andersen, I. Stensgaard, R. Feidenhansl, J. E. Sorensen, *Phys. Rev. Lett.* **1982**, *49*, 669.
[16] J. W. M. Frenken, J. F. Vanderveen, *Phys. Rev. Lett.* **1985**, *54*, 134.
[17] J. W. M. Frenken, P. M. J. Maree, J. F. Vanderveen, *Phys. Rev. B* **1986**, *34*, 7506.
[18] R. Zivieri, G. Santoro, V. Bortolani, *Phys. Rev. B* **2000**, *62*, 9985.
[19] V. B. Nascimento, E. A. Soares, V. E. de Carvalho, E. L. Lopes, R. Paniago, C. M. C. de Castilho, *Phys. Rev. B* **2003**, *68*, 245408.
[20] R. Paule, J. Mandel, *Pure Appl. Chem.* **1972**, *31*, 395.
[21] J. R. Sambles, L. M. Skinner, Lisgarte. Nd, *Proc. R. Soc. Lond. Ser. A* **1970**, *318*, 507.
[22] C. C. Chou, J. L. McAtee, *Clay Clay Miner.* **1969**, *17*, 339.
[23] Y. Khalavka, C. Ohm, L. Sun, F. Banhart, C. Sonnichsen, *J. Phys. Chem. C* **2007**, *111*, 12886.
[24] T. Castro, R. Reifenberger, E. Choi, R. P. Andres, *Phys. Rev. B* **1990**, *42*, 8548.
[25] P. Buffat, J. P. Borel, *Phys. Rev. A* **1976**, *13*, 2287.
[26] Y. G. Sun, Y. N. Xia, *Science* **2002**, *298*, 2176.

Received: July 7, 2009
Revised: September 10, 2009
Published online: October 30, 2009

